SUPPLEMENTARY INFORMATION

Absolute $^{13}C/^{12}C$ Isotope Amount Ratio for Vienna Pee Dee Belemnite from Infrared Absorption Spectroscopy

Adam J. Fleisher[1,4,✉], Hongming Yi[1,4,5], Abneesh Srivastava[1], Oleg L. Polyansky[2,3], Nikolai F. Zobov[3], and Joseph T. Hodges[1]

[1]Material Measurement Laboratory, National Institute of Standards and Technology, Gaithersburg, MD, USA

[2]Department of Physics and Astronomy, University College London, London, UK

[3]Institute of Applied Physics, Russian Academy of Sciences, Nizhny Novgorod, Russia

[4]These authors contributed equally: Adam J. Fleisher, Hongming Yi

[5]Present affiliation: The Department of Civil and Environmental Engineering, Princeton University, Princeton, NJ, USA

✉To whom correspondence should be addressed: adam.fleisher@nist.gov

S1. Spectroscopic model and reference data. For the evaluation of $R(^{13}C/^{12}C)_{sample}$, the spectroscopic model comprised reference data for the transition frequencies (ν), total internal partition sums [$Q(T)$], upper-state statistical weight (g'), and lower-state rotational energies (E'') taken from the HITRAN2016 database[1]. Known weaker CO_2 transitions within the 12 GHz tuning range centered about each targeted transition were included in the spectroscopic model using Voigt line shape profiles, but with fixed spectroscopic parameters based on the known gas sample molar fraction [$\chi(CO_2)$] and measured temperature (T) and pressure (p). No significant water absorption was observed in any of the spectral regions of interest. All isolated target transitions were modeled using a speed-dependent Nelkin-Ghatak line shape profile[2,3]. Weak $^{13}C^{16}O_2$ interferences from the presence of trace methanol (CH_3OH)[4] within the CRDS cell were also included in the fit when necessary, typically only after long sample residence times of >2 h. Therefore, individual static gas sample charges were rarely measured for longer than 2 h, thus avoiding substantial CH_3OH interferences.

Spectroscopic reference data for the targeted CO_2 transitions is summarized in Table S1. For $^{13}C^{16}O_2$, the transition intensities (S) were calculated from an updated *ab initio* dipole moment surface (DMS) and semi-empirical potential energy surface (PES) as detailed in the Methods section. For $^{12}C^{16}O_2$, values of S were taken from the broadband experimental work of Long et al.[5] which followed initial multi-instrument comparisons of a single transition by Fleisher et al.[6]. Those accurate $^{12}C^{16}O_2$ intensities were determined with traceability to measurements of time, frequency, temperature, pressure, and gravimetrically assigned mole fraction. We emphasize that our values of $R(^{13}C/^{12}C)_{VPDB}$ inferred from infrared absorption spectroscopy will scale inversely with the ratios of intensities, s_r, as described by Eq. **[2]** in the main text.

Table S1. Summary of spectroscopic reference data used to calculate $R(^{13}C/^{12}C)_{sample}$ from the observed integrated line areas, a.

Isotope	Upper vibrational state $(v_1 v_2 \ell_2 v_3 r)$	Rotational state	Transition frequency $(\tilde{\nu})$ cm^{-1}	Upper state degeneracy (g')	Lower state rotational energy (E'') cm^{-1}	Isotopic-abundance normalized transition intensity (S_{I_a}) [a] cm molecule^{-1}	Transition intensity (S) [b] cm molecule^{-1}
$^{13}C^{16}O_2$	20011	R 12e	5000.855475	54	60.8738	7.584×10^{-24}	6.859×10^{-22}
$^{13}C^{16}O_2$	20011	R 18e	5004.842483	78	133.4456	7.754×10^{-24}	7.012×10^{-22}
$^{12}C^{16}O_2$	30012	R 16e	6359.967244	35	106.1297	1.7607×10^{-23}	1.7890×10^{-23}
$^{12}C^{16}O_2$	30012	R 18e	6361.250350	39	133.4393	1.7221×10^{-23}	1.7497×10^{-23}

[a] Calculated with HITRAN isotope abundances[1]: $^{13}C^{16}O_2$, 0.011057; $^{12}C^{16}O_2$, 0.984204.
[b] Transition intensities, S, for $^{13}C^{16}O_2$ were calculate here from the quantum chemistry methods described in the Methods section. Values of S for $^{12}C^{16}O_2$ were taken from Long et al.[6].

S2. Quantifying uncertainty in the quantum chemistry calculations. The benchmarking of quantum chemistry theory against highly accurate experimental measurements of S is an active area of research[1,5-15]. Using quantum chemistry methods, Lodi and Tennyson[16] developed a method of estimation which, when applied to CO_2[7], resulted in an upper-bound relative standard uncertainty of 5×10^{-3}. To further estimate the uncertainty in our $^{13}C^{16}O_2$ intensities predicted by the updated *ab initio* DMS and semi-empirical PES, we compare predicted $^{12}C^{16}O_2$ intensities with highly accurate experimental results in the literature. Tables S2 and S3 list $^{12}C^{16}O_2$ near-infrared transition intensities for R 12e and R 18e lines from both theory and experiment.

Table S2. Comparison between theory and experiment for near-infrared R 12e $^{12}C^{16}O_2$ lines.

Wave number cm^{-1}	Upper vibrational state $(v_1 v_2 \ell_2 v_3 r)$	Line intensity from experiment (S_{exp}) cm molecule^{-1}	Reference	Line intensity from HITRAN2016 (S_{HT16}) cm molecule^{-1}	Line intensity from updated calculations (S_{theory}) cm molecule^{-1}	HITRAN2016 relative to updated calculations $(\frac{S_{HT16}}{S_{theory}} - 1)$ 10^{-3}	Experiment relative to updated calculation $(\frac{S_{exp}}{S_{theory}} - 1)$ 10^{-3}
4863.398	20013	2.6364×10^{-22}	15	2.618×10^{-22}	2.6173×10^{-22}	0.4	7.3
4987.308	20012	1.2748×10^{-21}	9	1.273×10^{-21}	1.2716×10^{-21}	1.2	2.5
5109.310	20011	--	--	4.171×10^{-22}	4.1592×10^{-22}	2.8	--
6085.882	30014	1.6542×10^{-24}	5	1.655×10^{-24}	1.6551×10^{-24}	0.1	−0.5
6237.421	30013	1.6831×10^{-23}	5	1.683×10^{-23}	1.6805×10^{-23}	1.2	1.5
6357.311	30012	1.7065×10^{-23}	5	1.724×10^{-23}	1.7165×10^{-23}	4.5	−5.8

Table S3. Comparison between theory and experiment for near-infrared R 18e $^{12}C^{16}O_2$ lines.

Wave number cm^{-1}	Upper vibrational state $(v_1 v_2 \ell_2 v_3 r)$	Line intensity from experiment (S_{exp}) cm molecule^{-1}	Reference	Line intensity from HITRAN2016 (S_{HT16}) cm molecule^{-1}	Line intensity from updated calculations (S_{theory}) cm molecule^{-1}	HITRAN2016 relative to updated calculations $(\frac{S_{HT16}}{S_{theory}} - 1)$ 10^{-3}	Experiment relative to updated calculation $(\frac{S_{exp}}{S_{theory}} - 1)$ 10^{-3}
4867.672	20013	2.7490×10^{-22}	15	2.730×10^{-22}	2.7292×10^{-22}	0.3	7.2
4991.258	20012	1.3188×10^{-21}	11	1.313×10^{-21}	1.3112×10^{-21}	1.2	5.8
5113.456	20011	--	--	4.253×10^{-22}	4.2420×10^{-22}	2.6	--
6090.294	30014	1.7323×10^{-24}	5	1.733×10^{-24}	1.7333×10^{-24}	0.1	−0.5
6241.402	30013	1.7481×10^{-23}	5	1.748×10^{-23}	1.7453×10^{-23}	1.3	1.6
6361.250	30012	1.7497×10^{-23}	5	1.768×10^{-23}	1.7595×10^{-23}	4.8	−5.6

For the R 12e lines (Table S2), the comparison between theory and experiment is plotted in Fig. S1. We estimate that the calculated CO_2 intensities reported here are accurate to within an equally probable range of $\pm 6.6 \times 10^{-3}$. Assuming a uniform distribution with range value of 6.6×10^{-3}, the estimated relative standard uncertainty for our updated *ab initio* transition intensities is $u = 3.8 \times 10^{-3}$. (A similar result is achieved using the R 18e lines in Table S3.) Finally, we note that an identical analysis of the calculated CO_2 intensities[7,8] tabulated in HITRAN2016[1] would yield a slightly higher value of $u_r = 5.0 \times 10^{-3}$—illustrating the apparent overall convergence of updated theory with accurate experiments[5,9,11,15].

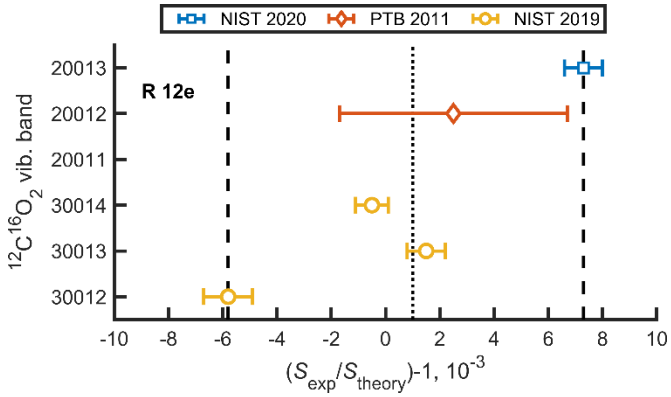

Fig. S1. Comparison between theory and experiment. The relative deviation between highly accurate experimental measurements[5,9,15] of R 12e CO_2 transition intensities and our updated quantum chemistry calculations. The dashed black lines indicate the bounds of an assumed uniform distribution with range parameter of 6.6×10^{-3}, and therefore $u = (6.6 \times 10^{-3})/\sqrt{3} = 3.8 \times 10^{-3}$. The dotted line is the average value of the uniform distribution, equal to 1.0×10^{-3}.

Previously[5,6], we have experimentally shown that CO_2 lines with peak absorbances per unit length equivalent to the 20011 ← 00001 transitions used here can be measured with relative combined uncertainty of $u_c < 0.1 \times 10^{-3}$. Therefore, similar measurements could be done for $^{13}C^{16}O_2$ line intensities if a gravimetrically prepared, isotopically enriched gas sample were available. Efforts to create just such a gas isotope reference material at NIST are underway. Furthermore, our updated *ab initio* DMS also suggests that accurate measurements of $^{12}C^{16}O_2$ lines within the 20011 ← 00001 band could be used to confirm predicted intensities for $^{13}C^{16}O_2$ as the underlying semi-empirical PES[17] has already been shown to perform well for both isotopologues. Analogous $^{13}C^{16}O_2$ calculations as those reported in Tables S2 and S3 showed identical trends relative to HITRAN2016 as those predicted for $^{12}C^{16}O_2$ (Tables S2 and S3, column 7), suggesting that the $^{13}C^{16}O_2$ predictions could be accurately scaled by any future measurements of the $^{12}C^{16}O_2$ isotopologue.

S3. Theory, mitigation, and uncertainty associated with temperature. At a given temperature, *T*, the transition intensity for each line is:

$$S(T) = \frac{A}{8\pi c\nu^2}\frac{g' e^{\frac{-E''}{k_B T}}}{Q(T)}\left\{1 - e^{\frac{-h\nu}{k_B T}}\right\}, \quad \text{(S1)}$$

where h is the Planck constant, c is the speed of light, k_B is the Boltzmann constant, ν is the transition frequency, A is the Einstein coefficient for spontaneous emission (proportional to $\mathcal{R}_m^2$, the transition dipole moment squared), g' is the upper-state statistical weight, E'' is the lower-state rotational energy, and $Q(T)$ is the total internal partition sum[1,18]. The terms (A, g', ν, E'') are physical invariants for a given molecule and absorption transition, while $Q(T)$ is a thermodynamic property of the corresponding molecular ensemble.

Because all infrared transitions studied here originated in the ground vibrational state of CO_2 and had characteristic transition wave numbers of $\tilde{\nu} = \nu/c \geq 5000$ cm^{-1} we could write $\frac{h\nu}{k_B T} \gg 1$, so that the line intensity ratio reduced to:

$$s_r(T) = \left\{\frac{A_1 g_1'/\nu_1}{A_2 g_2'/\nu_2}\right\}\left\{\frac{Q_2(T)}{Q_1(T)}\ e^{\frac{-h}{k_B T}[E_1'' - E_2'']}\right\}, \quad \text{(S2)}$$

where the subscripts 1 and 2 correspond to the $^{13}C^{16}O_2$ and $^{12}C^{16}O_2$ transitions, respectively. The temperature dependence of s_r was effectively eliminated by the choice of transitions pairs with nearly identical E'' listed in Table S1, i.e. $e^{\frac{-h}{k_B T}[E_1'' - E_2'']} \approx 1$ in Eq. (S2).

For most of the studied transition pairs, the magnitude of the temperature sensitivity was less than 0.8×10^{-3} K^{-1}. Given our maximum temperate uncertainty of 0.05 K, based on the

quadrature addition of a 0.02 K systematic uncertainty of the thermometer and 0.04 K uncertainty associated with temperature fluctuations during a scan, the unaccounted-for temperature effect on $R(^{13}C/^{12}C)_{VPDB}$ was at most 0.04×10^{-3} of our reported value.

S4. Validation of VPDB-CO_2 δ ^{13}C value assignments. A summary of our CO_2-in-air sample composition metrics is available in Table S4. In addition to the dual-inlet isotope ratio mass spectrometry (DI-IRMS) measurements[19], continuous-flow IRMS (CF-IRMS), developed for the study of CO_2-in-air samples directly from compressed gas cylinders, was utilized to compare all five CO_2-in-air samples following preparation. Preliminary CF-IRMS measurements confirmed the DI-IRMS assignments of the parent CO_2 gas samples at a relative level of 0.1 ‰.

Table S4. Sample CO_2 molar fractions [$\chi(CO_2)$] and isotope VPDB-CO_2 δ values. Combined standard uncertainties are shown in parentheses. Samples 1-4 were value-assigned at NIST via DI-IRMS. Also listed are the number of acquisition (n) per samples, where each n comprised 10 DI-IRMS cycles, and the number of AIR-IS acquisitions (N) per sample.

Sample	$\chi(CO_2)$ µmol/mol	u µmol/mol	Parent CO_2 DI-IRMS derived mean δ values				Notes
			δ ^{13}C ‰	δ ^{18}O ‰	n	N	
1	400.10	8	−2.18(6)	−16.0(3)	16	41	Sample AL2 of Ref. 19
2	399.53	8	−25.06(5)	−33.5(2)	11	59	Sample AL3 of Ref. 19
3	373.35	0.16	−32.56(5)	−23.7(3)	3	80	Protocol from Ref. 19
4	437.4	0.9	−39.63(5)	−30.6(3)	5	52	Protocol from Ref. 19
5	393.23	0.07	−8.6(0)	−1.1(1)	--	69	NIST SRM 1720 [a]

[a] The $\chi(CO_2)$ value was measured by NIST[20]. The δ ^{13}C value was measured by the NOAA Earth Systems Research Laboratory, Global Monitoring Division, Central Calibration Laboratory: https://www.esrl.noaa.gov/gmd/ccl/refgas.html, search Serial Number CC324315

The uncertainty associated with the NIST IRMS value assignments of VPDB-CO_2 δ ^{13}C had a minimal impact on the absolute isotope amount ratio $R(^{13}C/^{12}C)_{VPDB}$ estimated in this work. Srivastava & Verkouteren[19] provided estimates of potential biases in the NIST IRMS value assignments (0.06 ‰, or 0.06×10^{-3}) which were within the Type B uncertainty values of the isotope reference materials NIST RM 8562, 8563 and 8564 employed for VPDB traceability. Furthermore, the δ ^{13}C uncertainties of 0.06×10^{-3} were well below the total combined relative uncertainty dominated by the AIR-IS instrumentation and available reference data.

Two biases (i.e., systematic uncertainty, Type B uncertainty) associated with IRMS value assignments will now be discussed. Firstly, the δ ^{13}C values depended upon the choice of ^{17}O parameters. In turn, the ^{17}O parameters depend upon the absolute isotope ratio of the reference material $R(^{13}C/^{12}C)_{VPDB}$. Contrasting the treatments of IAEA[21] and IUPAC[22] where assumed values for $R(^{13}C/^{12}C)_{VPDB}$ differed by 5.1×10^{-3}, a δ ^{13}C value assignment bias of ≤0.05 ‰ was estimated across the −25.06 ‰ to 1.85 ‰ isotope range. In summary, the effect of the assumed value of $R(^{13}C/^{12}C)_{VPDB}$ on the ^{17}O parameters resulted in an estimated δ ^{13}C value assignment uncertainty of ≤0.05 ‰[23].

Secondly, potential biases in the DI-IRMS measurements was evaluated via a null hypothesis test of isotope reference materials (RMs) NIST RM 8562, 8563 and 8564[20,23], whereby two of the isotopic RM were treated as unknowns and the remaining one isotopic RM was used for VPDB-CO_2 δ ^{13}C scale realization (i.e., single-point scale realization). The null hypothesis tests resulted in an estimated 0.04 ‰ uncertainty, again within the Type B uncertainty of the isotopic RMs.

In summary, the combined relative standard uncertainty associated with IRMS $\delta^{13}C$ value assignments at NIST was ≈0.06 ‰ (calculated from the quadrature sum of 0.05 ‰ and 0.04 ‰), a minor uncertainty contribution when compared to the combined relative standard uncertainty of 3.9×10^{-3} reported in the main text and dominated by the optical measurement and reference data uncertainties.

S5. Choice of distribution function to represent the $R(^{13}C/^{12}C)_{VPDB}$ data set. Portions of Fig. 3 of the main text are reproduced below as Fig. S2, and a complete set of references is included in Fig. S2C[24-30]. Related to Fig. S2C, note that the mean value of $R(^{13}C/^{12}C)_{VPDB}$ calculated from the available sample of seven independent measurements (Refs. 25-30 plus this work) is $R(^{13}C/^{12}C)_{VPDB}$ = 0.011118 with an expanded uncertainty, U_{95} = 0.000034, estimated from the standard error of the mean, u_c = 0.000014, multiplied by the 95 % coverage factor for six degrees of freedom, k_{95} = 2.45.

For this work, we report in the main text $R(^{13}C/^{12}C)_{VPDB}$ calculated from the mean value of our 301 measurements. Here we assess variation associated with the choice of the distribution function or the weighting of the individual measurement points to extract the mean value from the data set. Firstly, we chose an empirical distribution function: a two-parameter Weibull distribution. The Weibull function was chosen to account for the observed bias-corrected skewness of −0.71 and kurtosis of 4.0 found in the fitted normal distribution function. We also compare the weighted mean and the median of the data set in Table S5.

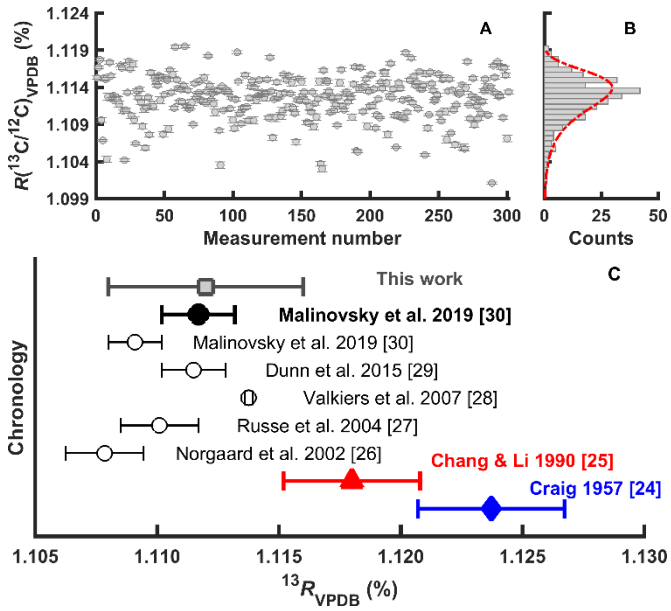

Fig. S2. A. Reproduction of the data series shown in Fig. 3A of the main text. **B.** Fitted two-parameter Weibull distribution as an alternative approach to extracting the data series mean value. **C.** Literature comparison like that shown in Fig. 3C of the main text, plotted here with additional references labeled. The black dot of Malinovsky et al.[30] is a best-estimate consensus value. The best-estimate mean value calculated from Ref. 25-30 and including this work is $R(^{13}C/^{12}C)_{VPDB}$ = 0.011118 with an expanded uncertainty of U_{95} = 0.000034.

Table S5. Characteristic values for the choice of distribution function of $R(^{13}C/^{12}C)_{VPDB}$ measurements plotted in Fig. S2A (reproduced from Fig. 3A of the main text). We report for $R(^{13}C/^{12}C)_{VPDB}$ the mean value from the normal distribution function plotted as a dashed-dotted red line in Fig. 3B of the main text.

Fitted distribution function	$R(^{13}C/^{12}C)_{VPDB}$	Standard error	Relative deviation from the fitted normal distribution (10^{-3})
Normal distribution	0.0111254	0.0000017	
Weibull distribution	0.0111244	0.0000019	−0.09
Weighted mean	0.011125	0.000002	−0.04
Median	0.0111285	0.0000016	0.28
Linear model [a]	0.011125	0.000005	0.04

[a] Fitted value of $R(^{13}C/^{12}C)_{VPDB}$ from the linear model plotted in red in Fig. 2A of the main text.

The largest relative deviation from the mean of the normal distribution is the median value, deviating by a relative amount of 0.28×10^{-3}. Assuming a uniform distribution with a range

parameter equal to this largest deviation, we estimate a relative standard uncertainty for the choice of distribution function to be equal to 0.16×10^{-3}. Compared to the other components comprising the uncertainty budget in Table 1 of the main text, this choice has a small effect.

References

1. Gordon I. E. et al. The HITRAN2016 molecular spectroscopic database. *J. Quant. Spectrosc. Radiat. Transfer* **203,** 3–69 (2017). doi:10.1016/j.jqsrt.2017.06.038
2. Nelkin, M. & Ghatak, A. Simple binary collision model for Van Hove's $G_s(r,t)$. *Phys. Rev.* **135,** A4 (1964). doi:10.1103/PhysRev.134.A4
3. Ciuryło, R., Pine, A. S. & Szudy, J. A generalized speed-dependent line profile combining soft and hard partially correlated Dicke-narrowing collisions. *J. Quant. Spectrosc. Radiat. Transfer* **68,** 257–271 (2001). doi:10.1016/S0022-4073(00)00024-8
4. Yi, H. & Fleisher, A.J. High-resolution cavity ring-down spectroscopy of the $\nu_1 + \nu_6$ combination band of methanol at 2.0 µm. *J. Chem. Phys.* **151,** 234202 (2019). doi:10.1063/1.5125146
5. Long, D. A. et al. High-accuracy near-infrared carbon dioxide intensity measurements to support remote sensing. *Geophys. Res. Lett.* **47,** e2019GL086344. doi:10.1029/2019GL086344
6. Fleisher, A. J. et al. Twenty-five-fold reduction in measurement uncertainty for a molecular line intensity. *Phys. Rev. Lett.* **123,** 043001 (2019). doi:10.1103/PhysRevLett.123.043001
7. Polyansky, O. L. et al. High-accuracy CO_2 line intensities determined from theory and experiment. *Phys. Rev. Lett.* **114,** 243001 (2015). doi:10.1103/PhysRevLett.114.243001
8. Zak, E. J. et al. Room temperature line lists for CO_2 symmetric isotopologues with *ab initio* computed intensities. *J. Quant. Spectrosc. Radiat. Transfer* **189,** 267–280 (2017). doi:10.1016/j.jqsrt.2016.11.022
9. Wübbeler, G., Víquez, G. J. P., Jousten, K., Werhahn, O. & Elster, C. Comparison and assessment of procedures for calculating the R(12) line strength of the $\nu_1 + 2\nu_2 + \nu_3$ band of CO_2. *J. Chem. Phys.* **135,** 204304 (2011). doi:10.1063/1.3662134
10. Odintsova, T. A. et al. Highly accurate intensity factors for pure CO_2 lines near 2 µm. *J. Chem. Phys.* **146,** 244309 (2017). doi:10.1063/1.4989925

11. Yi, H., Liu, Q., Gameson, L., Fleisher, A. J. & Hodges, J. T. High-accuracy $^{12}C^{16}O_2$ line intensities in the 2 µm wavelength region measured by frequency-stabilized cavity ring-down spectroscopy. *J. Quant. Spectrosc. Radiat. Transfer* **206,** 367–377 (2018). doi:10.1016/j.jqsrt.2017.12.008

12. Kang, P. et al. Line intensities of the 30011e – 00001e band of $^{12}C^{16}O_2$ by laser-locked cavity ring-down spectroscopy. *J. Quant. Spectrosc. Radiat. Transfer* **207,** 1–7 (2018). doi:10.1016/j.jqsrt.2017.12.013

13. Guay, P., Genest, J. & Fleisher, A. J. Precision spectroscopy of $H^{13}CN$ using a free-running, all-fiber dual electro-optic frequency comb system. *Opt. Lett.* **43,** 1407–1410 (2018). doi:10.1364/OL.43.001407

14. Makhnev, V. Yu. et al. A new spectroscopically-determined potential energy surface and ab initio dipole moment surface for high accuracy HCN intensity calculations. *J. Mol. Spectrosc.* **353,** 40–53 (2018). doi:10.1016/j.jms.2018.09.002

15. Fleurbaey, H., Yi, H., Adkins, E. M., Fleisher, A. J. & Hodges, J. T. Cavity ring-down spectroscopy of CO_2 near λ = 2.06 µm: Accurate transition intensities for the Orbiting Carbon Observatory-2 (OCO-2) "strong band." *J. Quant. Spectrosc. Radiat. Transfer* **252,** 107104 (2020). doi:10.1016/j.jqsrt.2020.107104

16. Lodi, L. & Tennyson, J. Line lists for $H_2{}^{18}O$ and $H_2{}^{17}O$ based on empirical line positions and *ab initio* intensities. *J. Quant. Spectrosc. Radiat. Transfer* **113,** 850-855 (2012). doi:10.1016/j.jqsrt.2012.02.023

17. Huang, X., Schwenke, D. W., Tashkun, S. A. & Lee, T. J. An isotopic-independent highly accurate potential energy surface for CO_2 isotopologues and an initial $^{12}C^{16}O_2$ infrared line list. *J. Chem. Phys.* **136,** 124311 (2012). doi:10.1063/1.3697540

18. Šimečková, M., Jacquemart, D., Rothman, L.S., Gamache, R. R. & Goldman, A. Einstein A-coefficients and statistical weights for molecular absorption transitions in the HITRAN database. *J. Quant. Spectrosc. Radiat. Transfer* **98,** 130-155 (2006). doi:10.1016/j.jqsrt.2005.07.003

19. Srivastava, A. & Verkouteren, R. M. Metrology for stable isotope reference materials: $^{13}C/^{12}C$ and $^{18}O/^{16}O$ isotope ratio value assignment of pure carbon dioxide gas samples on the Vienna PeeDee Belemnite-CO_2 scale using dual-inlet mass spectrometry. *Anal. Bioanal. Chem.* **410,** 4153–4163 (2018). doi:10.1007/s00216-018-1064-0

20. Rhoderick, G. C. et al. Development of a Northern Continental Air Standard Reference Material. *Anal. Chem.* **88,** 3376–3385 (2016). doi:10.1021/acs.analchem.6b00123

21. Allison, C. E., Francey, R. J. & Meijer, H. A. J. Recommendation for the reporting of stable isotope measurements of carbon and oxygen in CO_2 gas. International Atomic Energy

Agency (IAEA, 1995), (Report No. IAEA-TECDOC--825). https://inis.iaea.org/search/search.aspx?orig_q=RN:27021343

22. Brand, W. A., Assonov, S. S. & Coplen, T. B. Correction for the ^{17}O interference in $\delta(^{13}C)$ measurements when analyzing CO_2 with stable isotope mass spectrometry (IUPAC Technical Report). *Pure Appl. Chem.* **82,** 1719–1733 (2010). doi:10.1351/PAC-REP-09-01-05

23. Verkouteren, R. M. & Klinedinst, D. B. Value assignment and uncertainty estimation of selected light stable isotope reference materials: RMs 8543-8545, RMs 8562-8564, and RM 8566. NIST Special Publication 260-149 (2004). https://www.nist.gov/document-10350

24. Craig, H. Isotopic standards for carbon and oxygen and correction factors for mass-spectrometric analysis of carbon dioxide. *Geochim. Cosmochim. Acta* **12,** 133–149 (1957). doi:10.1016/0016-7037(57)90024-8

25. Chang, T. L. & Li, W.-J. A calibrated measurement of the atomic weight of carbon. *Chin. Sci. Bull.* **35,** 290–296 (1990). doi:10.1360/sb1990-35-4-290

26. Nørgaard, J. V. et al. The International Measurement Evaluation Program, IMEP-8: carbon and oxygen isotope ratios in CO_2. *Anal. Bioanal. Chem.* **374,** 1147-1154 (2002). doi:10.1007/s00216-002-1572-8

27. Ruße, K., Valkiers, S. & Taylor, P. D. P. Synthetic isotope mixtures for the calibration of isotope amount ratio measurements of carbon. *Int. J. Mass. Spec.* **235,** 255-262 (2004). doi:10.1016/j.ijms.2004.05.007

28. Valkiers, S. et al. Preparation of synthetic isotope mixtures for the calibration of carbon and oxygen isotope ratio measurements (in carbon dioxide) to the SI. *Int. J. Mass. Spec.* **264,** 10-21 (2007). doi:10.1016/j.ijms.2007.03.012

29. Dunn, P. J. H., Malinovsky, D. & Goenaga-Infante, H. Calibration strategies for the determination of stable carbon absolute isotope ratios in a glycine candidate reference material by element analyser-isotope ratio mass spectrometry. *Anal. Bioanal. Chem.* **407,** 3169-3180 (2015). doi:10.1007/s00216-014-7926-1

30. Malinovsky, D., Dunn, P. J. H., Holcombe, G., Cowen, S. & Goenaga-Infante, H. Development and characterization of new glycine certified reference materials for SI-traceable $^{13}C/^{12}C$ isotope amount ratio measurements. *J. Anal. At. Spectrom.* **34,** 147-159 (2019). doi:10.1039/c8ja00281a